

Infrared Tracers of Mass-Loss Histories and Wind-ISM Interactions in Hot Star Nebulae

Patrick Morris¹ and the *Spitzer* WRRINGS team

¹NASA Herschel Science Center, IPAC, Caltech, M/C 100-22, Pasadena, CA 91125
 email: pmorris@ipac.caltech.edu

Abstract. Infrared observations of hot massive stars and their environments provide a detailed picture of mass loss histories, dust formation, and dynamical interactions with the local stellar medium that can be unique to the thermal regime. We have acquired new infrared spectroscopy and imaging with the sensitive instruments onboard the *Spitzer* Space Telescope in guaranteed and open time programs comprised of some of the best known examples of hot stars with circumstellar nebulae, supplementing with unpublished Infrared Space Observatory spectroscopy. Here we present highlights of our work on the environment around the extreme P Cygni-type star HDE316285, providing some defining characteristics of the star's evolution and interactions with the ISM at unprecedented detail in the infrared.

Keywords. stars: mass loss, (stars:) circumstellar matter, stars: winds, outflows, infrared: stars

1. Introduction

Observations of the circumstellar environments of Luminous Blue Variables (LBVs) with ESA's Infrared Space Observatory (ISO) and modern ground-based imaging devices have demonstrated how sensitive mid-infrared imaging and spectroscopy can substantially improve our knowledge of the distribution of material, the physical and chemical properties of nebular dust and gas, and therefore on the history of mass loss from the surface of the massive central star during its evolution from the Main Sequence. Other than the bright and compact environments of most LBV nebulae, none of the lower surface brightness nebulae around OB or Wolf-Rayet stars could be observed with ISO due mainly to instrumental sensitivity limitations. The instruments on the *Spitzer* Space Telescope have since offered significant gains in sensitivity and sky coverage; for comparison, the *Spitzer* Infrared Spectrometer (IRS; 5.3 – 38 μm) is factor of ~ 50 -100 more sensitive than the ISO Short Wavelength Spectrograph (SWS; 2.4-45.2 μm) at 5 μm , depending on resolution modes of the two instruments. We have exploited the *Spitzer* IRS, the Infrared Array Camera (IRAC) with imaging bands at 3.4, 4.6, 5.8, and 8.0 μm , and the Multiband Imaging Photometer for *Spitzer* (MIPS) with imaging capabilities at 24, 70, and 160 μm in Guaranteed and Open Time programs to observe the environments around a number of hot, massive stars. Most of these stars are surrounded by ring nebulae and are well known for their optical and/or radio properties; NGC2359 (WR), M1-67 (WR), G79.29+00.46 (BIe), and HD148937 (Ofp?e) are examples.

In this paper we summarize our study of the massive B supergiant and candidate LBV HDE316285 from our program. This highly luminous P Cyg-type star has been suspected of being surrounded by an extended, cold nebula (McGregor, Hyland, & Hillier 1998); we have obtained conclusive observations of the environment around this star, which harbor telling characteristics of the star's mass loss history, wind-wind and wind-ISM interactions, the molecular content of the gas and thermal history of the dust.

2. The ring nebula around the extreme P Cygni star HDE316285

The combined 1.4-38 μm spectrum of HDE316285 is shown in Fig. 1. This star has been quantitatively characterized by Hiller et al. (1998) using line-blanketed non-LTE wind models as an “extreme” P Cygni-type star, with an optical and near-IR stellar wind spectrum that is quite similar to that of P Cyg. Spectral variability, the stellar properties and chemical content of HDE 316285 are similar to known LBVs, but is more extreme than P Cyg because of its high wind performance number (= ratio of wind momentum to radiative momentum), some 30 times greater. This number, however, is based on the assumption of a smooth, homogeneous wind and is subject to downward revision in the case of a clumped wind and associated reduction to the mass loss rate (cf. Hillier&Miller 1999). Somewhat unexpectedly, however, the infrared continuum, which can be used to constrain the volume filling factor (e.g., Morris et al. 2000), is contaminated by a strong thermal excess which becomes evident at around 16 μm (see Fig. 1). In fact McGregor, Hyland, & Hillier (1988) had pointed out that HDE316285 is a moderate IRAS source, exhibiting cold dust (~ 60 K) removed from the central star. Since this star is projected $\sim 1^\circ$ from the Galactic Center and is now recognized to be in close (apparent) proximity to the infrared star forming region (SFR) Sgr D (discussed below), a significant thermal component arising from surround molecular material heated by nearby young stars would provide the most likely explanation for the excess emission in the IRAS 25 and 60 μm passbands.

Infrared imaging. We now confirm that HDE316285 is definitely surrounded by its own circumstellar nebula. Following careful inspection of archival Midcourse Space Experiment 21.3 μm data in which a bipolar nebula can be seen just barely above the detection threshold, our MIPS 24 μm imaging (see Fig. 2) reveals a limb-brightened, $3'.4 \times 4'.1$ ring nebula with the major axis oriented $\sim 40^\circ$ from the north. The nebula is *not* discernable overall in the IRAC bands, though one bright knot of 8.0 μm emission is detected $\sim 1'$ NE of the central star. This knot and the brightened southern limb (respectively labelled “2” and “1” in Fig. 1) exhibit peak nebular fluxes of 624 and 450 MJy/sr, and were targeted by us for IRS spectroscopy, shown in Fig. 2 and discussed below. The nebula at 24 μm also clearly exhibits a clumpy structure, and filaments directed radially outwards

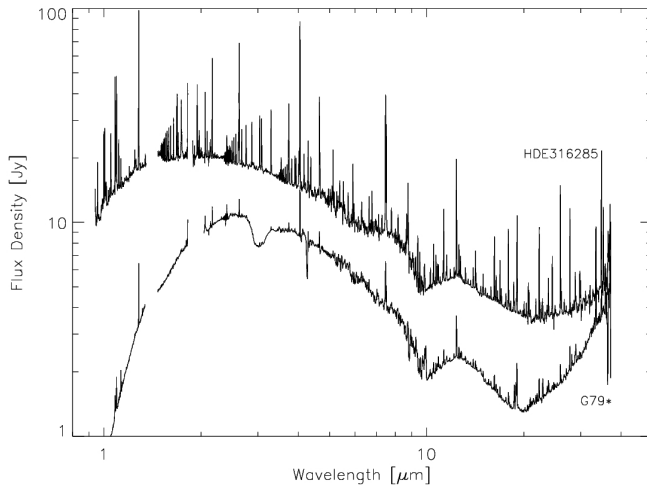


Figure 1. Combined near-IR (1.4-2.4 μm), ISO/SWS (2.4-10 μm), and *Spitzer*/IRS (10.0-38 μm) SEDs of HDE316285 (upper) and G79.29+00.46 (lower). From Morris et al. (2008) submitted.

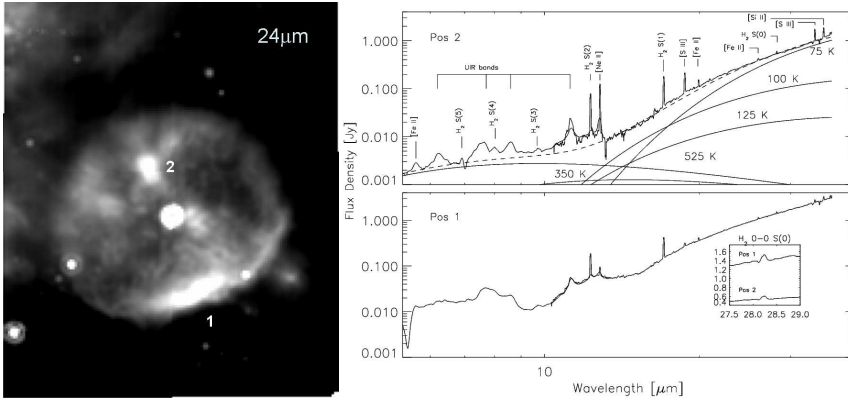


Figure 2. *Left:* HDE316285 at 24 μm with Spitzer/MIPS. The image is $5'.5 \times 8$, north is up, east is left. Two regions targeted for spectroscopy are indicated. *Right:* IRS 5.3-38 μm spectra at two positions in the nebula (background-subtracted), with main features identified.

particularly evident in the NE half. The SW rim of the nebula appears to be interacting with material emitting at 8.0 μm in the surrounding ISM. (see also Fig. 3).

Spectral content: PAHs and rotational H_2 . Spectra extracted at the two positions indicated in Fig. 2 and fully corrected for background emission with a dedicated off-position observation reveal thermal spectra with two principle components: a dominant cool component in the 75-125 K range, and a warm component at $T_{\text{dust}} > 350$ K. Atop the warm component we see the family of polyaromatic hydrocarbon (PAH) bands at 6.22, 7.63, 8.63, 11.22, and 12.75 μm , and possibly a number of secondary peaks. These bands are common in reflection nebulae and the shells of AGB and post-AGB stars with mixed C and O chemistries, but they have also been detected mixed with the crystalline silicate dust in the nebulae around LBVs AG Car and R71 (Voors et al. 1999, 2000). We return to these features at the end of this paper.

The HDE316285 nebular spectra also exhibit pure rotational lines of H_2 arising from optically thin quadrupole transitions, from S(0) at 28.3 μm through S(6) at 6.1 μm , though the S(4) 8.0 μm and S(6) lines are blended with PAH emission. *This is the first known detection of rotational transitions of H_2 in the nebula of a hot massive star.* St. Louis et al. (1998) have previously detected the ro-vibrational 1-0 S(1) 2.112 μm line in the NGC2359 nebula around WR7, in a region where the nebula may be interacting with a surrounding bow shock. From this single line, however, St. Louis et al. could not deduce the excitation mechanism. This is relevant to the debate on the contribution of hot stars to the H_2 luminosity in starburst galaxies and ULIRGs, where fluorescent excitation in the UV radiation fields of OB and WR stars has been generally preferred over collisionally-induced emission for lack of cases of the latter in local settings.

The H_2 rotational lines are readily thermalized at moderate volume densities, allowing us to estimate H_2 column densities and excitation temperatures under the assumption of LTE in order to gain insight into the excitation conditions of the line forming regions. We follow excitation diagram methods developed by Burton (1992) and Gredel (1994), and applied to comparable environments (as in, e.g., NGC7129 by Morris et al. 2004 and references therein). The column density for transition j is $N_j = 4\pi F_j / \Omega E_j g_j A_j$, where E_j is the energy of the upper level, g_j is the statistical weight of ortho- and para-transitions, and A_j is the transition probability. The line column density is related to the total column density and excitation temperature T_{ex} by $\ln(N_j/g_j) = \ln(N_{\text{tot}}/Q) - E_j/(kT_{\text{ex}})$, and may be solved for with a Boltzmann excitation diagram. The partition function Q was

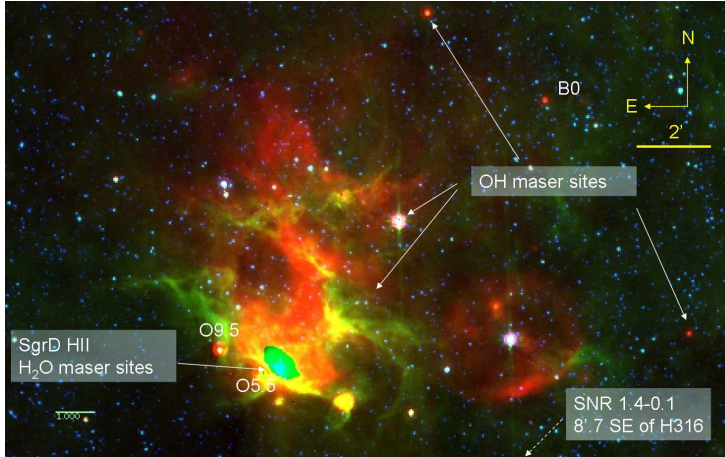


Figure 3. Mosaic of the Sgr D region, with radio sources identified by Mehringer et al. (1998) indicated. Blue corresponds to 4.6 μm , green to 8.0 μm , and red to 24 μm .

determined with an ortho-para ratio of 3 under the assumption of thermal equilibrium. For the observed line fluxes per unit solid angle F_j/Ω , we have extracted over regions of 40 arcsec² and 62 arcsec² in the 5.3 – 14 μm and 14 – 35 μm ranges, respectively. In these areas we must view our measurements as spatially integrated. The measured line intensities were corrected for reddening $A_V = 6.0$ mag (Hillier et al. 1998). Measurement uncertainties of the S(3) – S(5) lines arise predominantly from the blending with the PAH features and the flux calibration. The S(6)/S(5) or S(4)/S(5) line ratios could be also affected by an ortho-para ratio different than the canonical (thermal equilibrium) value of 3, as in the presence of shocks, or by the superposition of multiple layers along the line of sight with different physical conditions. From our computed values of $\ln(N_j/g_j)$ and E_{up}/K we obtain estimates of the total H₂ column density $N_{\text{tot}} \simeq 1.5 \times 10^{20} \text{cm}^{-2}$ and excitation temperature $T_{\text{ex}} \simeq 240$ K, averaged over the two positions.

The relatively low value of T_{ex} at the high H₂ column density (compared to typical photodissociation regions) seem quite reasonable for line emission in the outflow arising from collisional (dissociative J-shock) excitation. We favor the J-shock mechanism over C-shocks in the outflow, based on the S(0) line intensity and strong [Si II] 34.815 μm emission. From J-shock models (Hollanbach & McKee 1989) we see also by the presence of [Ne II] 12.81 μm that the velocity is probably greater than 50 km sec⁻¹.

Is HDE316285 a hyper-luminous counterpart of the Pistol Star? In order to estimate the physical size and age of the nebula around HDE316285 we must know the distance to the star. Hillier et al. (1998) adopted 2 kpc, as a rough average of literature values between 1 and 3.4 kpc, and conceded that there is no real constraint on the distance. At that time it was not recognized that HDE316285 lies in close (apparent) proximity to the infrared SFR Sgr D (see Fig. 3). Assuming HDE316285 to be equidistant with Sgr D has the appeal of placing this B supergiant in the same dynamic ecosystem as the SFR and neighboring YSOs and maser sources, as well as a supernova remnant SNR 1.4-0.1 a few arcmin to the SE. Mehringer et al. (1998) have estimated the distance of Sgr D as 8 kpc based on H₂CO and CS line kinematics measured at the VLA. At this distance, the stellar luminosity of HDE316285 must be corrected from $\log(L_*/L_\odot) = 5.5$ to 6.7! This takes into account a small reduction to $T_{\text{eff}} (\simeq 14\text{kK})$ in the most recent line-blanketed models, but does very little to moderate *a stellar luminosity matched only by the Pistol Star in the GC and η Carina*. Assuming a distance of 8 kpc, then the diameter of the

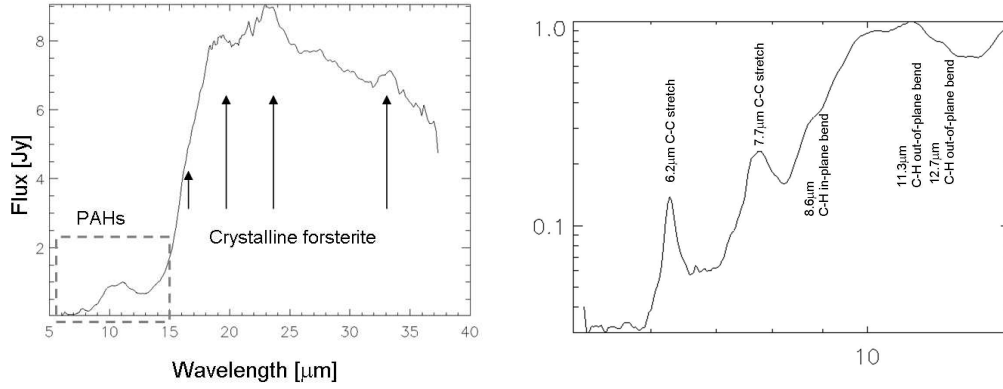


Figure 4. *Left:* *Spitzer*/IRS spectrum of the LMC LBV R71, with principle crystalline silicate bands and PAH features indicated. Nebular dust properties have been studied by Voors et al. (1999) using ISO/SWS data to 25 μm . *Right:* Zoom on the PAH bands in the IRS spectrum. Was the material comprised of crystalline dust and hydrocarbons condensed in the C-rich envelope of an RSG phase?

nebula is 8.6 pc, and must have a dynamical age of at least 9300 years using an upper constraint of 450 km/s for the time-averaged expansion velocity set by the unresolved IRS lines ($\lambda/\Delta\lambda \simeq 650$).

We cannot settle comfortably with this new distance to HDE316285, unfortunately. Blum & Damineli (1999) have presented K-band imaging of Sgr D, from which they argue that the SFR is located between 4-7.9 kpc (for $d_{GC} = 8$ kpc) and suggest $A_K = 1.9$ mag from the nebular Br- γ /radio flux ratio. No point sources are detected in the K-band image within the core of Sgr D, but focusing on sources within a few arcmin of the SFR, 18 of 34 sources have $A_K \leq 1.5$ mag (versus $A_K = 3$ for the GC itself). They devised a model with a uniform $A_K = 2.2$ mag screen of extinction at 4 kpc from the Sun, matching the actual star counts. HDE316285 has $A_V = 8$ mag ($A_K \sim 0.8$ mag), which is substantially lower, suggesting that the star is in the foreground. Indeed, University College London Echelle Spectrograph data taken in May 1995 show NaI D velocities of around +5 km/s, in agreement with a low distance to HDE316285 from comparison with the Brand & Blitz (1993) rotation curve using $d_{GC} = 8$ kpc.

In summary, we are confronted with conflicting evidence on the distance to Sgr D and HDE316285: on the one hand H_2CO and CS radio line kinematics place Sgr D at 8 kpc, while near-IR modeling of the reddened star population close to SFR can satisfy observed star counts at half the distance. Admittedly the latter method involves many more approximations and ensuing uncertainties, but the optical line (Na D) kinematics and comparatively low reddening of HDE316285 taken at their face values do not favor a large distance. If the B supergiant star is in the foreground, between 2 and 4 kpc, then either a substantial amount of foreground material is present also in the immediate surrounding ISM to interact with the stellar outflow, or else the H_2 lines are being formed in collisions between the present-day stellar wind and the outflow detected in our 24 μm observations.

Implications and Outlook. The fact that HDE316285 is surrounded by a bipolar nebula supports the notion suggested by Hillier et al. (1998) that this luminous, strong-winded B supergiant has recently passed through an LBV phase. This is more plausible at a lower

distance to the star with a commensurately lower limit age of the nebula, (i.e., ≥ 2300). We have also noted the lack of specific dust bands that are the signatures of crystalline material which normally condenses in the thick, slowly-expanding envelopes of RSGs, suggesting that the material forming the present-day nebula was rapidly ejected and could not crystallize under conditions of rapid cooling and low monomer densities. The explosive outflows from η Carina also lack crystalline silicates, though there are a number of dust bands in this N-rich, C-depleted environment which are yet to be properly identified (Morris et al. 1999). In contrast, ISO spectroscopy of the LBVs AG Car, WRA 751, and R71 (Voors et al. 1999, 2000) reveal crystalline properties of the O-rich dust and the presence of C-rich hydrocarbons. See Fig. 4 for the IRS spectrum of R71. These properties are more consistent with formation during a RSG phase, supplying appropriate temperature and density condensation conditions as well as surface chemistries in which $N(C)/N(O) > 1$, and fits with the rather low outflow velocities and time-averaged mass-loss rates which yield the nebular masses estimated by Voors et al.

We must be careful to consider certain potential attenuating effects on dust crystallinity when interpreting the mass-loss history. Specifically, silicates initially condensed amorphously in an eruption might be annealed under electron bombardment (Carrez et al. 2002a). Forsterite, an Mg-rich crystalline silicate detected in the aforementioned LBVs (see Fig. 4), can be formed at fluences of $\sim 10^{17} \text{ e}^-/\text{cm}^2$ where (in the laboratory) particles are accelerated to several 10^6 eV . This may occur in YSOs with magnetic fields. OB supergiants are not magnetically active (except in the rare Ofp?e cases) and therefore the mechanism of electron bombardment would require acceleration by other means. Conversely, amorphization of initially crystalline dust may occur under heavy proton bombardment, which may explain the lack of crystalline silicates in the ISM (Carrez et al. 2002b, Brucato et al. 2004). Both effects of electron (re-)annealing and proton amorphization require study applied to BSG/RSG environments in order to improve the use of dust grain properties as tracers of the evolutionary state of the underlying star during condensation.

References

- Blum, R. D., & Damineli, A. 1999, *apj*, 512, 237
 Brand, J., & Blitz, L. 1993, *A&A*, 275, 67
 Brucato, J. R., Strazzulla, G., Baratta, G., & Colangeli, L. 2004, *A&A*, 413, 395
 Burton, M. G. 1992, *AuJPh*, 45, 463
 Carrez, P., et al. 2002a, *Meteoritics & Plan. Sci.*, 37, 1615
 Carrez, P., et al. 2002, *Meteoritics & Plan. Sci.*, 37, 1599
 Gredel, R. 1994, *A&A*, 292, 580
 Hillier, D. J., & Miller, D. L. 1999, *ApJ*, 519, 354
 Hillier, D. J., Crowther, P. A., Najarro, F., & Fullerton, A. W. 1998, *A&A*, 340, 483
 McGregor, P. J., Hyland, A. R., & Hillier, D. J. 1988, *ApJ*, 324, 1071
 Mehringer, D. M., Goss, W. M., Lis, D. C., Palmer, P., & Menten, K. M. 1998, *ApJ*, 493, 274
 Morris, P. W., et al. 1999, *Nature*, 402, 502
 Morris, P. W., et al. 2000, *A&A*, 353, 624
 Morris, P. W., et al. 2004, *ApJS*, 154, 339
 St-Louis, N., Doyon, R., Chagnon, F., & Nadeau, D. 1998, *AJ*, 115, 2475
 Voors, R. H. M., et al. 1999, *A&A*, 341, L67
 Voors, R. H. M., et al. 2000, *A&A*, 356, 501

Discussion